Monolayer single-crystal 1T'-$MoTe_2$ grown by chemical vapor deposition exhibits a weak antilocalization effect

Carl H. Naylor*[1], William M. Parkin[1], Jinglei Ping[1], Zhaoli Gao[1], Yu Ren Zhou[1], Youngkuk Kim[2], Frank Streller[3], Robert W. Carpick[3], Andrew M. Rappe[2], Marija Drndic[1], James M. Kikkawa[1], A. T. Charlie Johnson*[1]

[1] *Department of Physics and Astronomy, University of Pennsylvania,*
[2] *Department of Chemistry, University of Pennsylvania,*
[3] *Department of Mechanical Engineering and Applied Mechanics, University of Pennsylvania, Philadelphia, Pennsylvania 19104, United States*

***Email:** naylorc@sas.upenn.edu, cjohnson@physics.upenn.edu

Supplementary XPS, Figure S1:

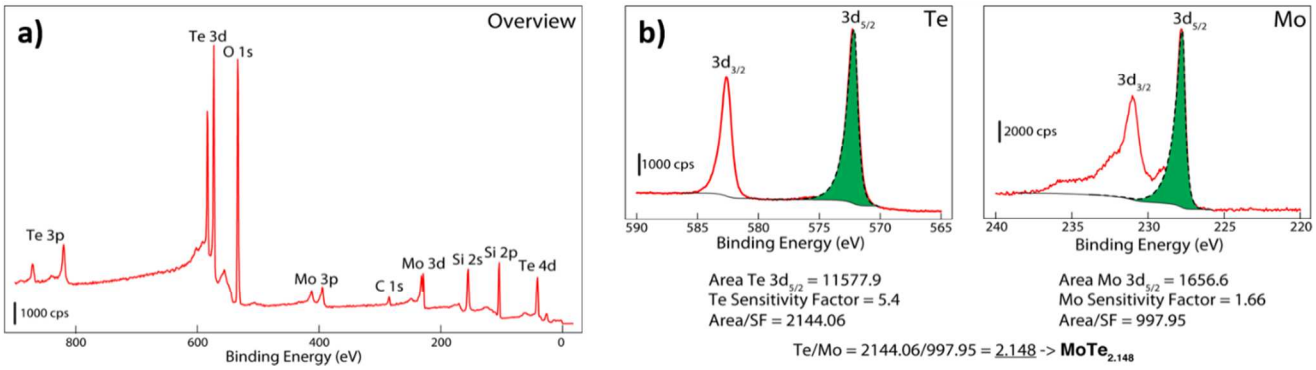

Figure S1: XPS data. a) Full XPS spectrum. b) Determining the stoichiometry of sample.

Supplementary Raman, Figure S2:

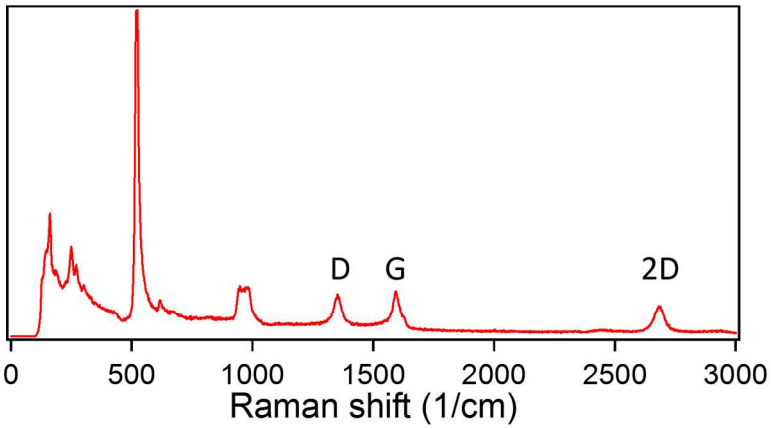

Figure S2: Raman data. Full Raman spectrum of graphene and $MoTe_2$. The presence of the graphene layer does not affect the Raman modes of $MoTe_2$, which appear in the range 112 – 269 cm^{-1}.

Supplementary TEM, Figures S3-S5:

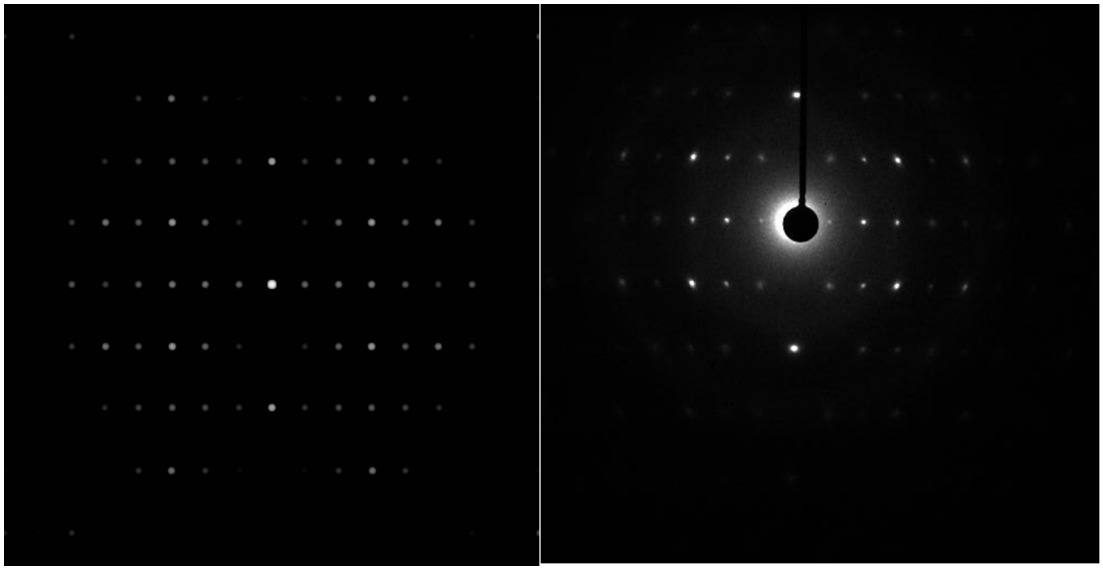

Figure S3 : Simulated (left) and experimental (right, also shown in Figure 3b of the main text) selected-area electron diffraction images for monolayer 1T'-$MoTe_2$. JEMS[1] was used to perform the simulation. It should be noted that the tilt within the $MoTe_2$ unit cell, which leads to only non-symmorphic symmetries and unambiguous $\vec{a}$ and $\vec{b}$ directions, could not be determined by SAED, so the directions of $\vec{a}$ and $\vec{b}$ and the reciprocal lattice directions discussed in the text are only good up to a negative sign.

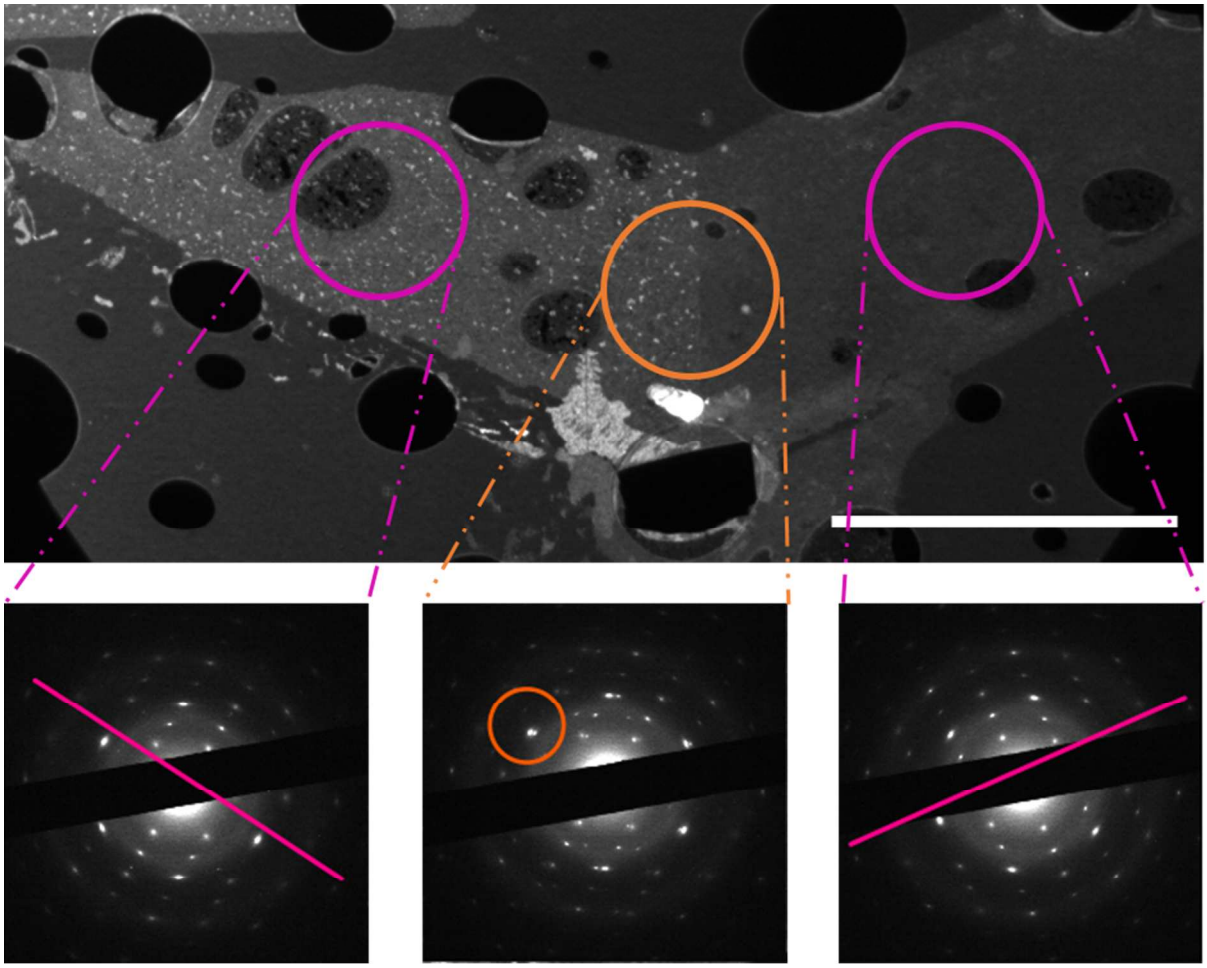

Figure S4: Dark field-TEM image (200 keV) of a polycrystalline $MoTe_2$ flake on a holey-carbon TEM grid. The scale bar is 2 µm. The SAED patterns on the left and right below the image show the relative crystal orientations of the two regions, which are separated by a tilt boundary with a crystal lattice rotation of 121.7° ± 0.5°. The central SAED pattern shows diffraction peaks associated with both domains. To form the image, an objective aperture was used to select an area around the (020) reflection of the flake's left leg and the (310) reflection of the flake's right leg, as indicated with the orange circle in the central SAED pattern. The crystallite on the left is brighter, as expected since simulations show that the intensity of the (020) reflection is greater than the (310) reflection by a factor of ~1.23. This tilt boundary was observed consistently across many polycrystalline flakes.

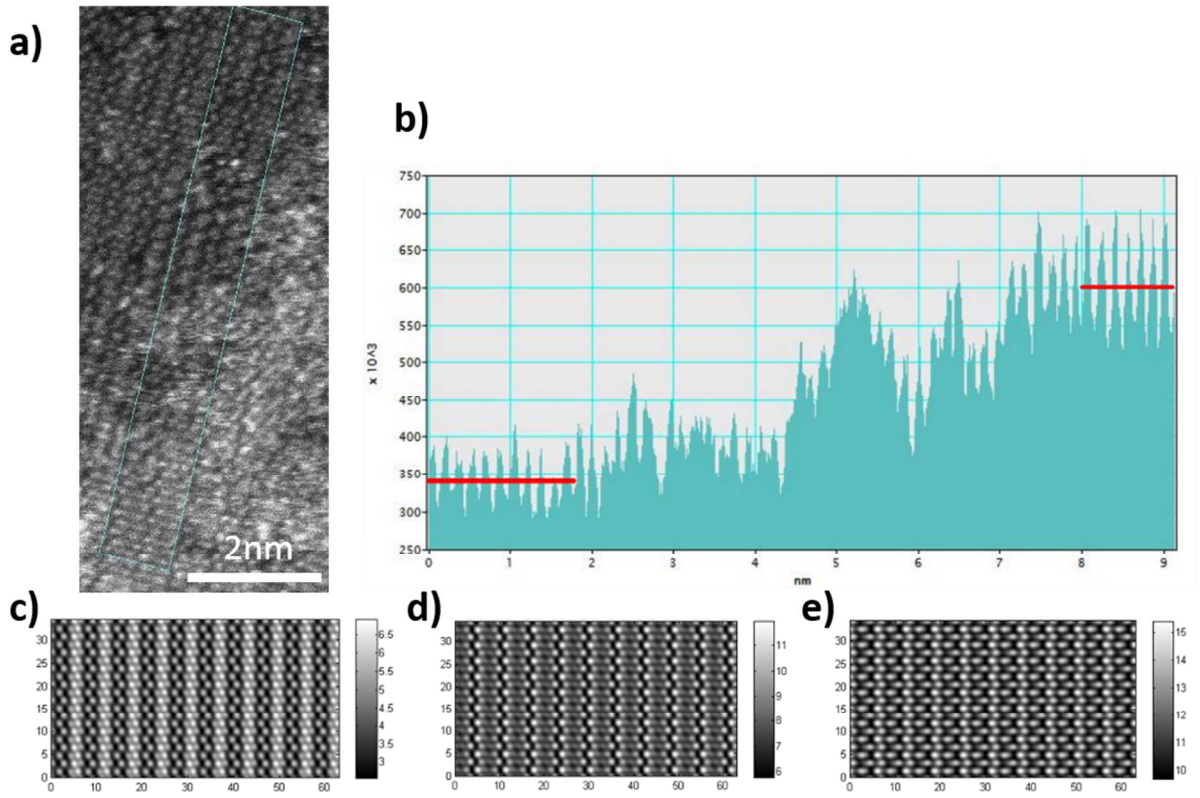

Figure S5: (a) Raw high-angle annular dark field (HAADF) image of an area containing monolayer and bi-layer regions. The bi-layer region is also shown in Figure 3e in the main text. (b) 100 pixel wide line scan from the monolayer region to the bi-layer region. The average pixel intensities for the mono- and bilayer regions are 3.45k and 6.06k, respectively, giving an intensity ratio of ~ 1.76. (c,d,e) Mono, bi, and tri-layer multislice HAADF simulated images. The average intensities of the simulated images are (in electrons times an arbitrary constant) 4.48, 8.10, and 11.81, respectively. The ratio of the bi-layer intensity to the monolayer intensity is 1.81, in good agreement with the experimental data. It should be noted that the disorder in the lattice is due to long exposure to atmosphere as well as damaged induced by the TEM beam.

Supplementary Electrical device 2, Figure S6:

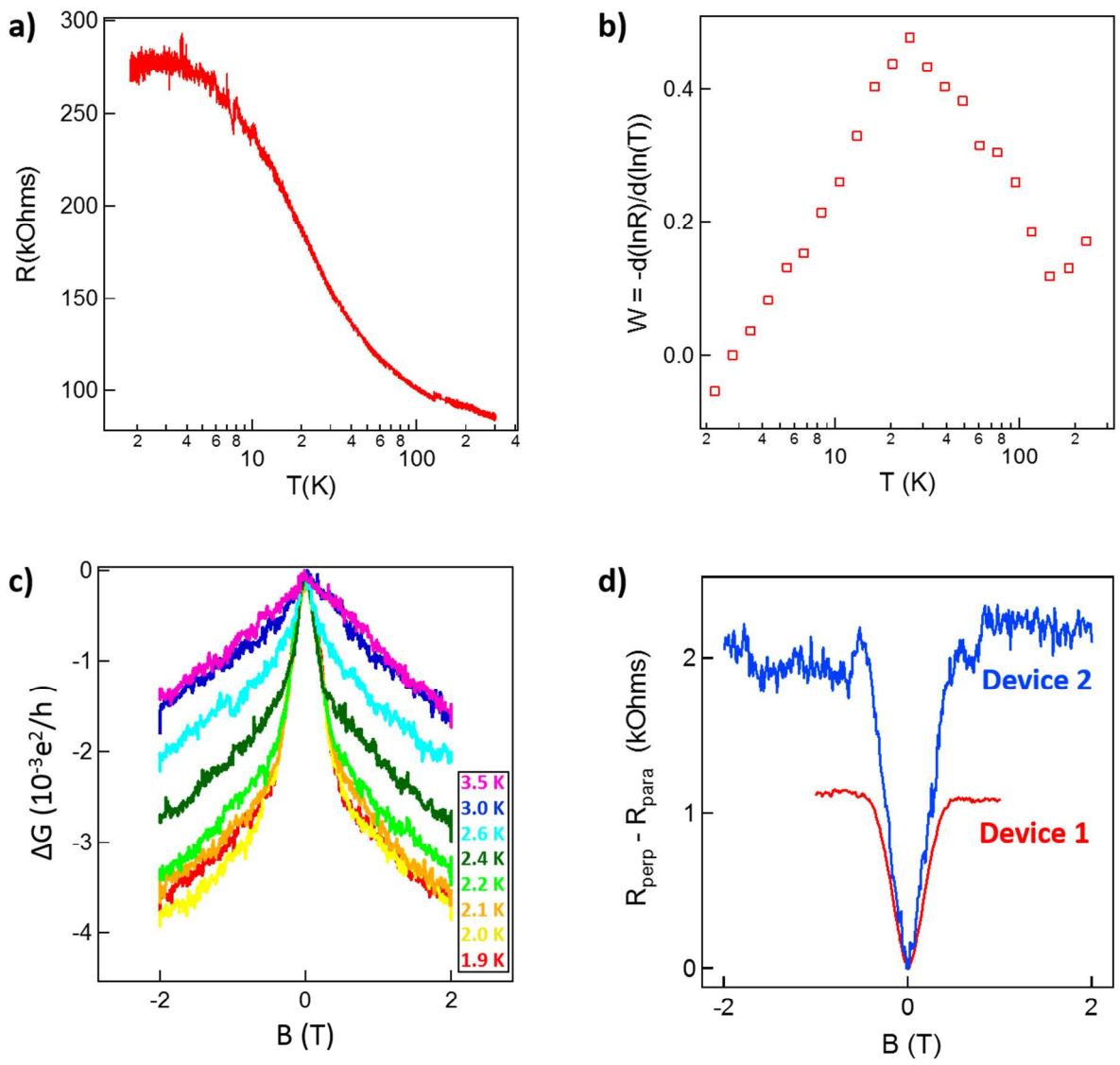

Figure S6: Electrical data for device 2. a) Sample resistance decreases with increasing temperature but the low temperature behavior is nevertheless metallic, as shown by the analysis in panel b. The magnitude of the WAL feature is much smaller for device 2 compared to the data presented in the main text, most likely due to a series resistance at the contacts. b) Reduced activation energy as a function of temperature showing a positive slope at low T, which is indicative of metallic behavior.[2] c) Magnetoconductance data at different temperatures showing the weak antilocalization (WAL) effect is also present in sample 2. The WAL feature weakens as the temperature is increased from 1.9 K to 3.5 K. d) $\Delta R(B)$ for device 1 and device 2, showing that the WAL effect on the resistance is very similar for the two samples.

Discussion about metastability of the material

The metastability in atmosphere of this material is evident, as we have noticed that leaving the sample exposed in air for several hours completely deteriorates the sample and the flakes are barely visible through an optical microscope. Furthermore, when the sample is exposed to the laser of our Raman system, we noticed that as we prolong the exposure time the peaks become less pronounced and then finally disappear. When graphene was added to the surface, the flakes became extremely stable under the Raman laser. This suggests that the $MoTe_2$ flakes quickly oxidize in atmosphere, but that the lattice is intrinsically stable.

Furthermore the raw AC STEM image reveals a large density of nanometer-sized holes as well as point defects in the lattice. The holes were due to the sample preparation for AC STEM, which required that the flakes be in ambient air for a couple of hours. We observed that the lattice crystal structure was preserved across all holes, which is strong evidence that the as-grown material is of very high structural quality, with the defects introduced by handling and exposure to air. Also, even at 80 kV operating voltage, we could see that the atoms were moving under irradiation and that the beam was introducing point defects and further deteriorating the sample. This indicates that the Mo and Te atoms are loosely bound and that the lattice is extremely sensitive to strain, and it is easy to simply detach parts of the crystals using the electron beam. These evidences confirm that 1T'-$MoTe_2$ is metastable and should be stored and treated appropriately.

Reference:

1. P. Stadelmann, JEMS—EMS Java version, CIME-EPFL, CH-1015 Lausanne, 2004.
2. Vora, P. M. et *al.* Correlating magnetotransport and diamagnetism of sp2–bonded carbon networks through the metal–insulator transition. *Phys. Rev. B* **2011**, 84, 155114.